HHS Public Access

Author manuscript

Sci Transl Med. Author manuscript; available in PMC 2019 February 21.

Published in final edited form as:

Sci Transl Med. 2018 February 21; 10(429): . doi:10.1126/scitranslmed.aam7729.

Oncogenic JAK2^{V617F} causes PD-L1 expression, mediating immune escape in myeloproliferative neoplasms

Alessandro Prestipino[1,2,†], **Alica J. Emhardt**[1,†], **Konrad Aumann**[3], **David O'Sullivan**[4], **Sivahari P. Gorantla**[1], **Sandra Duquesne**[1], **Wolfgang Melchinger**[1], **Lukas Braun**[1], **Slavica Vuckovic**[5], **Melanie Boerries**[6,7], **Hauke Busch**[6,8], **Sebastian Halbach**[6], **Sandra Pennisi**[1,2], **Teresa Poggio**[1], **Petya Apostolova**[1,9], **Pia Veratti**[1,7], **Michael Hettich**[10], **Gabriele Niedermann**[10], **Mark Bartholomä**[11], **Khalid Shoumariyeh**[1], **Jonas S. Jutzi**[1,2,12], **Julius Wehrle**[1,7,9], **Christine Dierks**[1], **Heiko Becker**[1], **Annette Schmitt-Graeff**[3], **Marie Follo**[1], **Dietmar Pfeifer**[1], **Jan Rohr**[13], **Sebastian Fuchs**[13], **Stephan Ehl**[13], **Frederike A. Hartl**[2,14], **Susana Minguet**[2,13,14], **Cornelius Miething**[1,7], **Florian H. Heidel**[15], **Nicolaus Kröger**[16], **Ioanna Triviai**[16], **Tilman Brummer**[6,7,14], **Jürgen Finke**[1], **Anna L. Illert**[1], **Eliana Ruggiero**[17],

[*]To whom correspondence should be addressed: Robert Zeiser, M.D., Department of Hematology and Oncology, Freiburg University Medical Center, Hugstetterstr. 55, 79106 Freiburg, Germany, Tel: (+49)0761270-34580, Fax: (+49)0761270-73570, robert.zeiser@uniklinik-freiburg.de.

[†]A.P. and A.J.E. contributed equally (co-first authors).

List of supplementary materials:

Author contributions: A.P. and A.E. helped to develop the overall concept, performed experiments, analyzed data and helped to write the manuscript, K.A. analyzed human BM-samples, D.O. performed metabolism experiments and analyzed data, S.P.G. helped with the JAK2 BM transfection model, S.D. and W.M. helped with multiple experiments, L.B. performed western blots, S.V. analyzed JAK2^{V617F}-mutant mice, M.B. and H.B. performed/analyzed array data, S.H. helped with transfection-experiments, S.P. analyzed peripheral blood-smears, T.P. performed transfection-experiments, P.A. collected patient data, P.V. helped with luciferase-promoter assay, M.H., M.B., G.N. performed/analyzed PET/CT-imaging, K.S. helped with luciferase-promoter-assays, J.J. helped with the Cre/lox-MPN-model, J.W. collected clinical data, C.D. provided help/vital reagents, H.B. collected clinical data, A.S.G. performed histology-analysis, M.F. helped with FACS/sorting-experiments, D.P. analyzed microarray-experiments and JAK2^{V617F}-allele burden, J.R., S.F., S.E. provided help with STAT-GOF/LOF, F.H. and S.M. helped with *in vitro* T-cell analyses, C.M. helped with luciferase-promoter assays, F.H. helped with EPO-R-tg 32D cells, N.K. and I.T. provided patient data, T.B. helped with cloning-experiments, J.F. provided patient data, L.I. supervised oncogene-cloning experiments, J.D., H.L.P. helped to plan/analyze experiments, E.R. and C.B. performed/analyzed TCR-sequencing. S.W.L. and G.H. provided JAK2-tg mice, supervised FACS-experiments, B.R.B. provided vital reagents/analyzed data, E.P. planned/analyzed metabolism experiments, R.Z. developed the overall study-concept/planned experiments, analyzed data and wrote the first draft of the manuscript.

Competing interests: The authors declare that they have no competing interests.

Data and materials availability: Microarray data are deposited in the database ArrayExpress (accession number E-MTAB-5028).

Chiara Bonini[17], **Justus Duyster**[1,7], **Heike L. Pahl**[1], **Steven W. Lane**[5,18], **Geoffrey R. Hill**[5,18], **Bruce R. Blazar**[19], **Nikolas von Bubnoff**[1,7], **Erika L. Pearce**[4], and **Robert Zeiser**[1,7,14,*]

[1]Department of Hematology and Oncology, Medical Center, University of Freiburg, Faculty of Medicine, Freiburg 79106, Germany

[2]Faculty of Biology, ALU-Freiburg 79104, Germany

[3]Institute of Surgical Pathology, Faculty of Medicine, University of Freiburg 79106, Germany

[4]Max Planck Institute for Immunobiology and Epigenetics, Freiburg 79108, Germany

[5]Department of Immunology, QIMR-Berghofer Medical Research Institute, Brisbane, QLD, Australia; and School of Medicine, University of Queensland, Herston, QLD 4006, Australia

[6]Institute of Molecular Medicine and Cell Research, Faculty of Medicine, University of Freiburg 79085, Germany

[7]German Cancer Consortium (DKTK), partner-site Freiburg; German Cancer Research-Center (DKFZ), Heidelberg 69120, Germany

[8]Institute of Experimental Dermatology, Institute of Cardiogenetics, University of Lübeck, Lübeck 23562, Germany

[9]Berta-Ottenstein-Programme, Faculty of Medicine 79106, University of Freiburg

[10]Department of Radiation Oncology, Faculty of Medicine, University of Freiburg, Freiburg 79106, Germany

[11]Department of Nuclear Medicine, University of Freiburg, Faculty of Medicine 79106, Germany

[12]Spemann Graduate School of Biology and Medicine (SGBM), University of Freiburg 79085, Germany

[13]Center for Chronic Immunodeficiency (CCI), Medical Center, University of Freiburg 79106, Germany

[14]Center for Biological Signalling Studies (BIOSS), University of Freiburg, Freiburg 79104, Germany

[15]Internal Medicine II, Hematology and Oncology, University Hospital of Jena, Germany and Leibniz-Institute on Aging (FLI) 07745, Jena

[16]Department of Stem Cell Transplantation, University Medical Center Hamburg-Eppendorf 20246, Germany

[17]Unit of Experimental Hematology, San Raffaele Scientific Institute, and University Vita-Salute San Raffaele, Milano 20132, Italy

[18]Royal Brisbane and Women's Hospital, Brisbane, QLD, University of Queensland, Herston, QLD 4072, Australia

[19]Department of Pediatrics, Division of Blood and Marrow Transplantation, University of Minnesota, Minneapolis 55455, USA

Abstract

Recent evidence has revealed that oncogenic mutations may confer immune escape. A better understanding of how an oncogenic mutation affects immunosuppressive PD-L1 expression may help in developing new therapeutic strategies. Here, we show that oncogenic JAK2 activity caused STAT3 and STAT5 phosphorylation, which enhanced PD-L1 promoter activity and PD-L1 protein expression in $JAK2^{V617F}$-mutant cells, whereas blockade of JAK2 reduced PD-L1 expression in myeloid $JAK2^{V617F}$-mutant cells. PD-L1 expression was higher on primary cells isolated from patients with $JAK2^{V617F}$-myeloproliferative neoplasms (MPN) compared to healthy individuals and declined upon JAK2 inhibition. $JAK2^{V617F}$ mutational burden, pSTAT3, and PD-L1 expression were highest in primary MPN patient-derived monocytes, megakaryocytes, and platelets. PD-1 inhibition prolonged survival in human MPN xenograft and primary murine MPN models. This effect was dependent on T cells. Mechanistically, PD-L1 surface expression in $JAK2^{V617F}$-mutant cells affected metabolism and cell cycle progression of T cells. In summary, we report that in MPN, constitutive JAK2/STAT3/STAT5 activation, mainly in monocytes, megakaryocytes, and platelets, caused PD-L1-mediated immune escape by reducing T cell activation, metabolic activity, and cell cycle progression. The susceptibility of $JAK2^{V617F}$-mutant MPN to PD-1 targeting paves the way for immunomodulatory approaches relying on PD-1 inhibition.

Introduction

Programmed death-ligand 1 and 2 (PD-L1, PD-L2) engage the programmed death receptor 1 (PD-1) on T cells and induce PD-1 signaling, which then causes multiple effects in T cells including exhaustion (1), alterations in glycolytic and mitochondrial metabolism (2), and reduced cell cycle activity (3). Tumor cells expressing PD-1 ligands on their surface use the PD-1 pathway to evade an effective antitumor immune response, and blockade of PD-1 is particularly effective in tumors with a high mutational burden (4). Genetic alterations including oncogenic activation of *Myc* (5) and loss of the tumor suppressor PTEN (6) cause increased PD-L1 expression (7).

JAK2 and PD-L1 are both localized on chromosome 9p.24. In Hodgkin's lymphoma patients, transcription of the PD-L1 gene is increased upon amplification of chromosome 9p24.1 (8–10). It was initially unclear if, comparable to the amplification of chromosome 9p24.1 causing higher JAK2 and PD-L1 copy numbers, oncogenic JAK2 activity also can induce PD-L1 expression and if so, whether this event is functionally causative for immune escape. A group of diseases characterized by oncogenic JAK2 activity are myeloproliferative neoplasms (MPN). The majority of MPN patients carry an activating point mutation in the JAK2 kinase ($JAK2^{V617F}$).

Because MPNs are potentially immunogenic neoplasms, as demonstrated by their susceptibility to interferon-α-2b (11) and detection of JAK2-specific T cells (12), we decided to clarify if there is a role for PD-L1 in this type of disease. We found that $JAK2^{V617F}$ activity causes STAT3 and STAT5 phosphorylation, which in turn enhances PD-L1 promoter activity and increases PD-L1 protein expression. Both in murine MPN models and in primary patient samples, megakaryocytes, monocytes, and platelets expressed PD-L1 more abundantly compared to either wildtype littermates or healthy individuals. Consistent

with the high PD-L1 expression observed, JAK2^{V617F}-MPN were susceptible to PD-1 blockade, which was dependent upon T cells, in a JAK2^{V617F}-driven mouse model, in human MPN xenografts, and in a MPN patient who relapsed after allogeneic hematopoietic cell transplantation (allo-HCT). Mechanistically, JAK2^{V617F}-mutant cells affected metabolism and cell cycle progression in Tcells via engagement with PD-L1 expressing mutant cells. Our findings identify a therapeutic concept for MPNs based on oncogene-driven immune escape via the JAK2/STAT3/STAT5/PD-L1 axis.

Results

JAK2 activation enhances PD-L1 expression via STAT3 phosphorylation

To test whether oncogenic JAK2 activity increases PD-L1 expression, we used a *Jak2*^{V617F} knock-in mouse model that develops polycythemia vera (13). In this model, we observed that PD-L1 surface expression was increased on megakaryocytes and monocytes derived from *Jak2*^{V617F} mice compared to *Jak2*-wild type (WT) littermate control mice (Fig. 1A, B, fig. S1). PD-L1 expression also increased in primary murine bone marrow (BM) cells upon transfection with a JAK2^{V617F} vector (Fig. 1C), indicating that JAK2 was responsible for the increase of PD-L1 surface expression in different cell types. The previously described FERM domain mutation (14), which causes oncogenic JAK2 activation (JAK2^{FERM}), also increased PD-L1 expression (Fig. 1D).

To understand the connection between oncogenic JAK2 and PD-L1, we transfected murine myeloid 32D cells with either a JAK2-WT vector or a JAK2^{V617F} vector (14). 32D cells are erythropoietin-dependent (15) and have high endogenous PD-L1 expression. In the absence of erythropoietin, PD-L1 expression is lower, and under these conditions PD-L1 expression increased in cells carrying the JAK2^{V617F} mutation (Fig. 1E, F). The same effects of mutant JAK2 on PD-L1 expression were seen in lymphoid Ba/F3 cells (fig. S2A, B).

Treatment with the JAK1/2 inhibitor ruxolitinib reduced PD-L1 expression in JAK2^{V617F}-mutant 32D cells (Fig. 1G, H) and Ba/F3 cells (fig. S2C). In contrast, when Ba/F3 cells contained a JAK2$^{V617F/L983F}$ mutation conferring ruxolitinib resistance, the PD-L1 expression declined less (fig. S2D). JAK2-specific inhibition with SD-1029 reduced PD-L1 expression in JAK2^{V617F}-mutant 32D (Fig. 1I) and Ba/F3 cells (fig. S2E, F) in a dose-dependent manner, without major cytotoxic effects at the concentrations applied (fig. S2G).

To test our hypothesis that JAK2 activation enhances PD-L1 promoter activity via STAT phosphorylation, we analyzed pSTAT1, pSTAT3, and pSTAT5 in the presence of oncogenic JAK2^{V617F}. Active tyrosine phosphorylated (p) STAT3 and pSTAT5 were increased in JAK2^{V617F}-mutant 32D cells compared to JAK2-WT 32D cells and to a lesser extent pSTAT1 also increased (Fig. 1J, K). In agreement with this, pSTAT3 was higher in JAK2^{V617F}Ba/F3 cells compared to empty-vector Ba/F3 cells (fig. S2H–K).

Then, to understand which pathway is involved in promoting PD-L1 expression, we made use of vectors expressing STAT proteins with gain of function (GOF) or loss of function (LOF) mutations. The STAT3-activating mutation Y640F (16) increased the expression of PD-L1 on 32D cells compared to STAT3-WT vector (Fig. 1L). A similar pattern was

observed in Ba/F3 cells with an activating STAT3 mutation (fig. S2L). Conversely, the STAT3 LOF mutations R382W and V637M reduced the expression of PD-L1 in JAK2^{V617F}-mutant 32D cells (Fig. 1M) and Ba/F3 cells (fig. S2M). Consistent with the idea that JAK2/STAT3 and PD-L1 are functionally connected, inhibition of STAT3 phosphorylation reduced PD-L1 expression (fig. S2N). Additionally, a STAT5 GOF mutation (17) caused increased PD-L1 expression, although to a lesser extent than the STAT3 GOF mutation (Fig. 1L). Consistent with a role for STAT5, the inhibition of STAT5 phosphorylation slightly reduced PD-L1 expression in 32D cells (fig. S2O) and Ba/F3 cells (fig. S2P). A STAT1 GOF mutation had no significant effect on PD-L1 expression (Fig. 1L). Our data are consistent with findings by others showing that STAT3 and STAT5 can bind the PD-L1 promoter (18).

To evaluate the concept that JAK2 inhibition blocks immune responses in MPN, we analyzed the amount of serum IFN-γ in mice bearing a JAK2^{V617F} MPN, which were treated with ruxolitinib or vehicle. We observed that ruxolitinib reduced IFN-γ (fig. S3). In light of these findings, it is likely that although therapeutic JAK2 inhibition will render MPN more immunogenic based on reduced PD-L1 expression, this intervention will at the same time counteract the T cell immune response against MPN.

In contrast to JAK2^{V617F}, other oncogenic mutations, including FLT3-ITD, FLT3-TKD, cKIT (d816v), EGFR (Del19, L861Q and L858R), or PDGFR (FIP1L1-PDGFRA), did not increase PD-L1 surface expression (fig. S4A, B). Because some of these mutations are found in acute myeloid leukemia (AML) (19, 20), we analyzed BM of AML patients and found that AML cells were mostly PD-L1 negative (fig. S4C, D). Consistently, pSTAT3 abundance was also low in primary human AML cells (fig. S4E, F).

JAK2 activation enhances PD-L1 expression in human cells

To evaluate whether the data obtained in murine cells were also applicable to human cells, we studied JAK2-WT or JAK2^{V617F} human cell lines. Transfection of K562 cells that express the ecotropic retrovirus receptor (21) with JAK2^{V617F} increased PD-L1 expression compared to empty vector cells (Fig. 2A, B). PD-L1 expression decreased upon JAK2 inhibition (Fig. 2C). Additionally, PD-L1 expression and pSTAT3 in different human JAK2^{V617F} cell lines (UKE-1, SET-2, MUTZ-8) could be reduced by specific JAK2 inhibition and ruxolitinib (Fig. 2D–L). We tested the activity of the PD-L1 promoter using luciferase reporter assays (fig. S5) in K562 cells. The activity of the PD-L1 promoter was higher in JAK2^{V617F}-mutant K562 cells compared to empty vector K562 cells (Fig. 2M). PD-L1 promoter activity declined upon JAK2 and STAT3 inhibition (Fig. 2N, O).

Additionally, we studied pSTAT1, pSTAT3, and pSTAT5 in K562 cells. We found that transfection of JAK2^{V617F} increased pSTAT3 and pSTAT5 but not pSTAT1 in K562 cells compared to empty vector (fig. S6A–C). A STAT1 GOF mutation did not increase PD-L1 expression in K562 cells, whereas PD-L1 increased in the presence of STAT3 GOF and STAT5 GOF mutations (fig. S6D).

Multiple cell types express increased PD-L1 in MPN patients

Next we analyzed PD-L1 expression on different primary human cells in the peripheral blood (PB) of MPN patients (patients' characteristics: table S1). PD-L1 expression on

peripheral blood cells and platelets was higher in $JAK2^{V617F}$ MPN patients compared to healthy volunteers (Fig. 3A, B). We observed that T cells, monocytes, myeloid-derived suppressor cells (MDSCs), and platelets all had higher PD-L1 expression in MPN patients compared to healthy controls (Fig. 3C). The slight increase of PD-L1 in human T cells and B cells in MPN patients compared to healthy controls (Fig. 3C) is consistent with reports by others that B and T cells in some patients with MPN also carry the V617F mutation (22). The high expression of PD-L1 on MDSCs and the previous report that MPN is also associated with increased numbers of MDSCs (23) point to immunosuppressive potential of these cells in MPN. In contrast to the $JAK2^{V617F}$ PBMCs, calreticulin (CALR) mutated PBMCs did not exhibit increased PD-L1 expression compared to cells derived from healthy individuals (fig. S7A). Cells with genomic amplification of JAK2 had increased PD-L1 expression (fig. S7B) and caused MPN-related death in a xenograft model, which could be prevented by anti-PD-1 therapy (fig. S7C).

Ruxolitinib treatment of MPN patients decreased PD-L1 expression on monocytes and platelets (Fig. 3D, E). Compatible with a causal connection between JAK2 activation, STAT3 phosphorylation, and PD-L1 expression, pSTAT3/STAT3 ratios decreased upon ruxolitinib treatment (Fig. 3F, G). Analysis of the BM from patients with different $JAK2^{V617F}$ MPN entities and healthy BM donors showed that MPN patients had higher numbers of $PD\text{-}L1^{+}$ cells and that the most common cell type expressing PD-L1 was the megakaryocyte (Fig. 3H–J).

Higher PD-L1 expression was associated with a more advanced MPN stage, as determined by histological signs and Dynamic International Prognostic Scoring System (DIPSS) score (24) (fig. S8A–C). MPN patients had lower CD4 and CD8 T cell numbers 5 years after diagnosis compared to MPN patients analyzed within the first year after diagnosis, suggesting that immunotherapy may be more effective in the earlier stages (fig. S8D).

We next transferred $JAK2^{V617F}$-transfected BM cells (BALB/c) into irradiated mice (BALB/c) and analyzed the distribution of PD-L1 in mice with $JAK2^{V617F}$-transfected BM that had developed MPN as evidenced by hematocrit and spleen size (fig. S9). PET combined with CT imaging of mice with $JAK2^{V617F}$-transfected compared to WT BM using a ^{64}Cu-labeled anti-PD-L1 antibody showed the highest PD-L1 expression in the spleen (Fig. 4A), which is an organ with a high disease burden in this MPN model. Mice with $JAK2^{V617F}$-transfected BM had higher PD-L1 expression (PET signal) in spleen and BM compared to WT-BM mice (Fig. 4B). This result supports our previous in vitro findings and flow cytometry analysis with in vivo real time data. Platelets had the highest PD-L1 expression in the $JAK2^{V617F}$-transfected BM MPN model (Fig. 4C, D). To verify these results in an additional model, we used an MPN model that relies on conditional expression of a $JAK2^{V617F}$-knock-in mutation in hematopoietic cells, activated via the Cre/lox system by crossing JAK2-L2 with Mx-Cre mice (JAK2-FLEX/+ or L2/+) (25). In this MPN model, we also observed that platelets had the highest expression of PD-L1 (Fig. 4E, F).

To understand why monocytes, platelets, and megakaryocytes have the highest PD-L1 expression, we studied the $JAK2^{V617F}$ allele burden in different cell types of MPN patients. We found that platelets and monocytes had a higher $JAK2^{V617F}$ allele burden than B cells, T

cells, or neutrophils from the same patients(Fig. 4G). We observed that human monocytes and platelets in the peripheral blood of MPN patients had higher pSTAT3 compared to B cells ($CD19^+$), T cells ($CD3^+$), or neutrophils ($CD15^+$) (Fig. 4H, I).

MPNs are susceptible to PD-1 inhibition in the context of T cells

Based on the high PD-L1 expression of human MPN cells, we next tested our hypothesis that this disease is susceptible to therapeutic PD-1 inhibition. We transferred human PBMCs from three MPN patients who had relapsed after allo-HCT (patient characteristics in table S2) into *RAG2*$^{-/-}$*Il2r*$^{-/-}$ mice and treated them with isotype IgG or anti-human PD-1 blocking antibody. *RAG2*$^{-/-}$*Il2r*$^{-/-}$ mice developed signs of MPN with increasing platelet counts (fig. S10A). We observed improved survival of mice treated with anti-PD-1 or anti-PD-L1 antibodies compared to mice treated with isotype IgG (Fig. 5A–C). Consistent with improved survival, we observed lower numbers of human platelets and $CD45^+$ cells in the peripheral blood of mice treated with anti-PD-1 antibody compared to those of mice treated with isotype IgG (Fig. 5D, E). Additionally, we found reduced numbers of human $CD45^+$ cells in BM of mice treated with anti-PD-1 antibody compared to those of mice treated with isotype IgG (Fig. 5F, G). Consistent with these findings, the $JAK2^{V617F}$ allele burden was lower in mice treated with anti-PD-1 antibody compared than in mice treated with isotype IgG (Fig. 5H). Immunohistochemistry-based analysis of the BM did not show a significant difference in human $CD45^+$ cells in mice treated with anti-PD-1 antibody compared to the isotype IgG-treated group (Fig. 5I, J).

The partial protection of mice treated with anti-PD-1 antibody compared to mice treated with isotype IgG was dependent on an intact donor T cell response, because depletion of $CD3^+$ T cells from the transferred PBMCs (fig. S10B) removed the survival advantage of mice treated with anti-PD-1 antibody compared to mice treated with isotype IgG (Fig. 5K). The GVHD histopathology scores for *RAG2*$^{-/-}$*Il2r*$^{-/-}$ mice that had received human MPN cells and human T cells were not different for mice treated with anti-PD-1 Ab or isotype IgG (fig. S10C).

To extend these results from the human xenograft model to another MPN model, we used the $JAK2^{V617F}$-transfected syngeneic BM model. After full engraftment and development of MPN, defined by a hematocrit over 60% in the PB, the mice underwent antibody treatment. Survival of mice treated with anti-mouse-PD-1 was improved compared to mice treated with isotype IgG (Fig. 5L). We observed that the ratio of effector/naive $CD8^+$ T cells increased in mice that were reconstituted with $JAK2^{V617F}$-transduced BM versus controls (Fig. 5M). This indicates that more effector T cells developed in these mice, which may have generated an anti-MPN effect. This effect was connected to PD-L1 expression because the ratio of effector/naive $CD8^+$ T cells increased further in mice treated with anti-mouse-PD-L1 compared to mice treated with isotype IgG (Fig. 5M). Shannon diversity index of complementarity determining region 3 amino acid sequences for TCR-α chains was significantly ($p=0.04$) lower in T cells of anti-PD-1-treated mice (Fig. 5N, O). These observations are in line with previous studies showing that T cell-mediated anti-leukemia response is linked to low TCR repertoire diversity (26).

PD-L1-expressing JAK2^{V617F} mutant cells affect cell cycle progression and metabolism in T cells

When T cells were exposed to JAK2^{V617F} myeloid 32D cells, unbiased gene expression analysis revealed down-regulation of multiple gene sets that represent metabolic pathways (Fig. 6A). One of the gene sets with reduced expression in T cells exposed to JAK2^{V617F} myeloid 32D cells was amino acid metabolism (Fig. 6A, asterisk). In agreement with this finding, murine T cells exposed to JAK2^{V617F} Ba/F3 cells showed down-regulation of genes related to methionine and cysteine metabolism, which are critical for T cell activation (27–29) (fig. S11A). The alanine serine and cysteine transporter system SLC1A5 (ASCT2), which was down-regulated in T cells upon exposure to JAK2^{V617F} Ba/F3 cells, is essential for T cell activation (30). Expression of SLC1A5 on T cells declined in a cell dose-dependent manner when they were exposed to JAK2^{V617F} Ba/F3 cells (fig. S11B). Consistent with our findings, a functional link between amino acid metabolism and PD-1 activation has been reported (2).

To understand if mutant JAK2-induced PD-L1 expression had an impact on T cell metabolism, we determined the rates of oxidative phosphorylation (OXPHOS) in CD3$^+$ T cells by measuring the oxygen consumption rate (OCR) at baseline and during a mitochondrial fitness test (31). Basal OCR in mouse CD3$^+$T cells was decreased after exposure to JAK2^{V617F}32D cells (Fig. 6B) or JAK2^{V617F}Ba/F3 cells (fig. S11C, D). Previous reports had shown that aerobic glycolysis is a hallmark of effector lymphocyte metabolism (31), which was reduced in the T cells exposed to the JAK2^{V617F}32D and JAK2^{V617F}Ba/F3 cells (Fig. 6B, fig. S11C, D). Because cell cycle progression is affected by PD-1 ligation on T cells, we next analyzed cell cycle-related genes. We observed that gene sets relevant for G1 to S phase transition were down-regulated in mouse T cells (isolated from C3H mice) that were exposed to JAK2^{V617F}32D (C3H background) cells (Fig. 6C). Cyclin-dependent kinase 6 (CDK6), which is required for cell cycle progression in T cells, was down-regulated in T cells exposed to JAK2^{V617F} Ba/F3 cells analyzed by gene expression array (fig. S11E). The gene expression of *Cdk8* was also down-regulated in T cells when JAK2^{V617F} Ba/F3 cells were present (fig. S11E). Conversely, gene expression of Cyclin G2 (*Ccng2*), which induces cell cycle arrest, and Cyclin-Dependent Kinase Inhibitor 2D (*Cdkn2d*), which reduces cell cycle activity, was upregulated in T cells exposed to JAK2^{V617F}Ba/F3 cells (fig. S11F). Consistently, we observed that the percentage of T cells in G0/G1 phase increased when T cells were exposed to JAK2^{V617F}Ba/F3 cells (fig. S11G). This pattern was not observed when the T cells were PD-1-deficient (fig. S11G), indicating that the effect was mediated via PD-1.

To understand if these findings could be reproduced in human cells, we co-cultured human T cells from healthy donors with JAK2^{V617F}K562 cells. Respiration in human CD3$^+$ T cells was decreased after exposure to JAK2^{V617F}K562 cells (Fig. 6D). Additionally, the percentage of T cells in G0/G1-phase increased when T cells were exposed to JAK2^{V617F}K562 cells (Fig. 6E).

Based on our findings in the mouse model, we treated patient #1 (table S2), who was initially diagnosed with polycythemia vera. He had undergone allo-HCT, relapsed, and was resistant to multiple salvage therapies (ruxolitinib, hydroxyurea, decitabine). The anti-PD-1

antibody nivolumab was used as an individualized approach. At the start of treatment, 98% of the $CD3^+$ cells were donor-derived, whereas 50% of the $CD34^+$ cells were recipient-derived (fig. S12A). Immunohistochemistry of the bone marrow showed the underlying MPN with a transformation into AML at the time of relapse. No additional mutations (besides $JAK2^{V617F}$) in the PBMCs were found by using a 48-gene myeloid panel sequencing approach that was confirmed by whole exome sequencing. In agreement with the findings in mice, in a patient with polycythemia vera we observed that recipient chimerism, $JAK2^{V617F}$ allele burden, $CD34^+$ cells in the peripheral blood, and cellularity in the BM all decreased after nivolumab treatment (fig. S12A–G). Conversely, the number of total $CD3^+$ cells in the PB increased after application of nivolumab (fig. S12H, I).

Based on our findings, we propose a scenario where oncogenic JAK2 activity results in STAT3 and STAT5 phosphorylation, which in turn enhances PD-L1 promoter activity (Fig. 6G). The cells carrying $JAK2^{V617F}$ express PD-L1 and thereby inhibit amino acid and glucose metabolism and cell cycle progression-promoting genes in T cells.

Discussion

Once a cell has acquired an oncogenic mutation allowing for uncontrolled proliferation and avoidance of apoptosis, a critical next step in the development towards neoplastic disease is to escape the immune system. Because both events, oncogenic transformation and immune escape, have to occur at the beginning of neoplastic development, it is likely that certain oncogenic mutations cooperate with mechanisms that allow immune escape. We found that oncogenic JAK2 activation results in high expression of PD-L1, mainly on the surface of monocytes, MDSCs, megakaryocytes, and platelets, and that this is mediated via the JAK2-STAT3 and JAK2-STAT5 axes. Consistent with our findings, others showed that pSTAT3 binds to and activates the PD-L1 gene promoter (32, 33). Because JAK2 is a canonical STAT3 activator and STAT3 activates PD-L1 transcription, the induction of PD-L1 in MPN was likely, and our study shows this connection experimentally in a systematic analysis of $JAK2^{V617F}$-mutant cells. Recently, a binding site for STAT5 was found in the *PD-L1* promoter region (18), but no functional connection between STAT5 activation and PD-L1 expression had been reported to date. We observed a minor role for STAT5 in PD-L1 expression, which was less prominent compared to the role of STAT3.

A limitation of the study is that we cannot clarify why AMLs do not exhibit high expression of PD-L1. A possible explanation is that other regulatory mechanisms for PD-L1 are active in AMLs. Interference with CMTM6 expression results in impaired PD-L1 protein expression because CMTM6 prevents PD-L1 from being targeted for lysosome-mediated degradation (34, 35). Therefore cells with a low amount of CMTM6 will have more PD-L1 degradation even if STAT3 activation is present. Another limitation of our study is that we used xenograft models of MPN, which are artificial because the recipient mice are immunodeficient. To correct for this, we had transferred T cells along with the MPN cells to allow for immune-mediated effects. An additional limitation is that our findings can only be applied to $JAK2^{V617F}$ mutant MPN, and we did not clarify which immune escape mechanisms are active in JAK2-negative MPN.

For a variety of tumor entities such as non-small cell lung cancer (36) and Hodgkin lymphoma (9), high expression of PD-L1 favors sensitivity of the malignancy to PD-1 inhibition. In particular, increased expression of PD-L1 on hematopoietic cells was associated with increased response (37). This is consistent with our finding showing that PD-L1 expression on cells was high in MPN, which then responded to PD-1 inhibition in an allo-HCT patient who had relapsed post-transplant. Previous work had shown that T cell-mediated immunosurveillance plays a central role in MPN progression, because T cells recognizing mutant JAK2 can be found in MPN patients (12), and MPNs are immunogenic because they respond to interferon-α-2b (11).

Our observation that PD-L1 expression is high on megakaryocytes is consistent with previous reports indicating that this cell type is an important disease-driving force in MPN (38, 39). However, other cell types, such as monocytes, MDSCs, and lymphocytes, expressed PD-L1, which is consistent with the fact that these cells also have a certain $JAK2^{V617F}$ allele burden (22). When murine or human T cells were exposed to $PD\text{-}L1^{high}$ cells with mutant JAK2, we observed major changes in metabolism, senescence, IFN-γ production, and cell cycle activity. In particular, cysteine metabolism was reduced when murine T cells were exposed to $PD\text{-}L1^{high}$ $JAK2^{V617F}$ cells. This may be a major mechanism for $JAK2^{V617F}$ cells to affect T cell activation because cysteine is the limiting precursor for glutathione synthesis, a prerequisite for antigen-dependent proliferation of T cells (29). The decreased OCR we observed in T cells exposed to $JAK2^{V617F}$ cells indicates that these T cells were overall less metabolically active, which is consistent with the idea that there is decreased cell cycle activity in this T cell population. Reduced proliferative capacity due to cell cycle inhibition may contribute to the reduced anti-tumor activity of T cells exposed to $PD\text{-}L1^{high}$ $JAK2^{V617F}$ cells. DNMT inhibitor treatment can also up-regulate PD-L1 expression in MDS, possibly causing disease resistance (40). Checkpoint inhibition can induce response rates above 50%, as recently reported for patients with different hematologic malignancies treated with an anti-CTLA-4 antibody after allo-HCT (41). We showed that activation of the JAK2/STAT3 and JAK2/STAT5 axes causes PD-L1-mediated immune escape in MPN. We defined megakaryocytes, platelets, and monocytes as the cell populations with the highest PD-L1 expression, and characterized a gene signature in T cells that were affected by the PD-L1-expressing cells. Furthermore, we reported the susceptibility of MPN to PD-1 inhibition, which should serve as a basis for immunotherapeutic approaches that rely on PD-1 inhibition in this disease entity.

Materials and Methods

Study design

For the sample size in the murine survival experiments, a power analysis was performed. A sample size of at least n=8 per group was determined to reach a statistical significance of 0.05 to detect an effect size of at least 1.06 with 80% power. Mice were assigned randomly to the experimental groups. All samples and mice were included in our analysis. Experiments were performed in a non-blinded fashion, except for the blinded GVHD severity scoring.

Human subjects

Human sample collection and analysis were approved by the Ethics committee of the University of Freiburg, Germany (protocol numbers: 10024/13, 558/15). Blood was collected from MPN patients or healthy volunteers after informed consent.

Statistical analysis

GraphPad-Prism v5.03 was used for statistical analysis. Normally distributed data were analyzed using the unpaired two-tailed *t*-test. When the data did not conform to a normal distribution, the Mann-Whitney *U* test was used. Differences in mouse survival (Kaplan-Meier survival curves) were analyzed by log-rank test. Data are presented as mean and SEM, unless otherwise indicated. A P value <0.05 was considered to be statistically significant.

Supplementary Material

Refer to Web version on PubMed Central for supplementary material.

Acknowledgments

Pd-1$^{-/-}$ mice on a C57BL/6 background were kindly provided by Prof. R. Schrimbeck (Universitätsklinikum Ulm, Germany). The conditional floxed JAK2 (*JAK2FLEX/+ or L2/+*) knock-in mice on C57Bl/6 background were a kind gift from Dr. Villeval (Inserm, U.1009, Villejuif, France).

Funding: This study was supported by ERC-Consolidator grant 681012 GvHDCure to RZ, DFG (Heisenberg-Professorship ZE872/3-2 to RZ, SFB1160/P14 to RZ, P1 to SE, SFB850/Z1 to H.B. and M.B., TRR167-NeuroMAC to RZ, EXC-306 to H.B. and MI1942/2-1 to S.M., DKH 111764 to NvB), Excellence-Initiative (DFG, GSC-4, SGBM) scholarship to J.J., MSCA-ITN-2015-ETN-ALKATRAS (A.-L.I.), NIH R01 CA72669 and P01 AI056299 to B.R.B., BMBF to M.B. and S.E. (e:Med research), BMBF 01EO1303, DeCaRe (FKZ 01ZX1409B), DFG 2508/4-1 (N.v.B.), Max-Planck-Society (E.P.). E. Ruggiero was supported by a fellowship by Associazione Italiana per la Ricerca sul Cancro (AIRC) co-funded by the European Union.

References and Notes

1. Tsushima F, Yao S, Shin T, Flies A, Flies S, Xu H, et al. Interaction between B7-H1 and PD-1 determines initiation and reversal of T-cell anergy. Blood. 2007; 110:180–185. [PubMed: 17289811]
2. Patsoukis N, Bardhan K, Chatterjee P, Sari D, Liu B, Bell LN, et al. PD-1 alters T-cell metabolic reprogramming by inhibiting glycolysis and promoting lipolysis and fatty acid oxidation. Nat Commun. 2015; 6:6692–6699. [PubMed: 25809635]
3. Latchman Y, Wood CR, Chernova T, Chaudhary D, Borde M, Chernova I, et al. PD-L2 is a second ligand for PD-1 and inhibits T cell activation. Nat Immunol. 2001; 3:261–268.
4. McGranahan N, Furness AJ, Rosenthal R, Ramskov S, Lyngaa R, Saini SK, et al. Clonal neoantigens elicit T cell immunoreactivity and sensitivity to immune checkpoint blockade. Science. 2016; 351:1463–1469. [PubMed: 26940869]
5. Casey SC, Tong L, Li Y, Do R, Walz S, Fitzgerald KN, et al. MYC regulates the antitumor immune response through CD47 and PD-L1. Science. 2016; 352:227–231. [PubMed: 26966191]
6. Parsa AT, Waldron JS, Panner A, Crane CA, Parney IF, Barry JJ, et al. Loss of tumor suppressor PTEN function increases B7-H1 expression and immunoresistance in glioma. Nature medicine. 2007; 13:84–88.
7. Kataoka K, Shiraishi Y, Takeda Y, Sakata S, Matsumoto M, Nagano S, et al. Aberrant PD-L1 expression through 3′-UTR disruption in multiple cancers. Nature. 2016; 534:402–406. [PubMed: 27281199]

8. Green MR, Monti S, Rodig SJ, et al. Integrative analysis reveals selective 9p24.1 amplification, increased PD-1 ligand expression, and further induction via JAK2 in nodular sclerosing Hodgkin lymphoma and primary mediastinal large B-cell lymphoma. Blood. 2010; 116:3268–3277. [PubMed: 20628145]
9. Ansell SM, Lesokhin AM, Borrello I, et al. PD-1 blockade with nivolumab in relapsed or refractory Hodgkin's lymphoma. N Engl J Med. 2015; 372:311–319. [PubMed: 25482239]
10. Roemer MG, Advani RH, Ligon AH, Natkunam Y, Redd RA, Homer H, et al. PD-L1 and PD-L2 Genetic Alterations Define Classical Hodgkin Lymphoma and Predict Outcome. J Clin Oncol. 2016; 34:2690–2697. [PubMed: 27069084]
11. Tichelli A, Gratwohl A, Berger C, Lori A, Würsch A, Dieterle A, et al. Treatment of thrombocytosis in myeloproliferative disorders with interferon alpha-2a. Blut. 1989; 58:15–19. [PubMed: 2644994]
12. Holmström MO, Hjortsø MD, Ahmad SM, Met Ö, Martinenaite E, Riley C, et al. The JAK2V617F mutation is a target for specific T-cells in the JAK2V617F positive myeloproliferative neoplasms. Leukemia. 2017; 31:495–498. [PubMed: 27761006]
13. Mullally A, Lane SW, Ball B, Megerdichian C, Okabe R, Al-Shahrour F, et al. Physiological Jak2V617F expression causes a lethal myeloproliferative neoplasm with differential effects on hematopoietic stem and progenitor cells. Cancer Cell. 2010; 17:584–596. [PubMed: 20541703]
14. Gorantla SP, Dechow TN, Grundler R, et al. Oncogenic JAK2V617F requires an intact SH2-like domain for constitutive activation and induction of a myeloproliferative disease in mice. Blood. 2010; 116:4600–4611. [PubMed: 20696946]
15. Schnöder TM, Arreba-Tutusaus P, Griehl I, Bullinger L, Buschbeck M, Lane SW, et al. Epo-induced erythroid maturation is dependent on Plcγ1 signaling. Cell Death Differ. 2015; 22:974–985. [PubMed: 25394487]
16. Flanagan SE, Haapaniemi E, Russell MA, Caswell R, Lango Allen H, De Franco E, et al. Activating germline mutations in STAT3 cause early-onset multi-organ autoimmune disease. Nat Genet. 2014; 46:812–814. [PubMed: 25038750]
17. Onishi M, Nosaka T, Misawa K, Mui AL, Gorman D, McMahon M, et al. Identification and characterization of a constitutively active STAT5 mutant that promotes cell proliferation. Mol Cell Biol. 1998; 18:3871–3879. [PubMed: 9632771]
18. Garcia-Diaz A, Shin DS, Moreno BH, Saco J, Escuin-Ordinas H, Rodriguez GA, et al. Interferon Receptor Signaling Pathways Regulating PD-L1 and PD-L2 Expression. Cell Rep. 2017; 19:1189–1201. [PubMed: 28494868]
19. Rombouts WJ, Blokland I, Lowenberg B, Ploemacher RE. Biological characteristics and prognosis of adult acute myeloid leukemia with internal tandem duplications in the Flt3 gene. Leukemia. 2000; 14:675–683. [PubMed: 10764154]
20. Allen C, Hills RK, Lamb K, Evans C, Tinsley S, Sellar R, et al. The importance of relative mutant level for evaluating impact on outcome of KIT, FLT3 and CBL mutations in core-binding factor acute myeloid leukemia. Leukemia. 2013; 27:1891–1901. [PubMed: 23783394]
21. Gerstmayer B, Groner B, Wels W, Schnierle BS. Stable expression of the ecotropic retrovirus receptor in amphotropic packaging cells facilitates the transfer of recombinant vectors and enhances the yield of retroviral particles. J Virol Methods. 1999; 81:71–75. [PubMed: 10488763]
22. Delhommeau F, Dupont S, Tonetti C, Massé A, Godin I, Le Couedic JP, et al. Evidence that the JAK2 G1849T (V617F) mutation occurs in a lymphomyeloid progenitor in polycythemia vera and idiopathic myelofibrosis. Blood. 2007; 109:71–77. [PubMed: 16954506]
23. Wang JC, Kundra A, Andrei M, Baptiste S, Chen C, Wong C, et al. Myeloid-derived suppressor cells in patients with myeloproliferative neoplasm. Leuk Res. 2016; 43:39–43. [PubMed: 26943702]
24. Passamonti F, Cervantes F, Vannucchi AM, Morra E, Rumi E, Pereira A, et al. A dynamic prognostic model to predict survival in primary myelofibrosis: a study by the IWG-MRT (International Working Group for Myeloproliferative Neoplasms Research and Treatment). Blood. 2010; 115:1703–1708. [PubMed: 20008785]

25. Hasan S, Lacout C, Marty C, Cuingnet M, Solary E, Vainchenker W, Villeval JL. JAK2V617F expression in mice amplifies early hematopoietic cells and gives them a competitive advantage that is hampered by IFNα. Blood. 2013; 122:1464–1477. [PubMed: 23863895]
26. Schultze-Florey C, Raha S, Ravens S, et al. TCR Diversity Is a Predictive Marker for Donor Lymphocyte Infusion Response. Blood. 2016; 128:4605.
27. Sido B, Braunstein J, Breitkreutz R, Herfarth C, Meuer SC. Thiol-mediated redox regulation of intestinal lamina propria T lymphocytes. J Exp Med. 2000; 192:907–912. [PubMed: 10993921]
28. Sikalidis AK. Amino acids and immune response: a role for cysteine, glutamine, phenylalanine, tryptophan and arginine in T-cell function and cancer? Pathol Oncol Res. 2015; 21:9–17. [PubMed: 25351939]
29. Sido B, Lasitschka F, Giese T, et al. A prominent role for mucosal cystine/cysteine metabolism in intestinal immunoregulation. Gastroenterology. 2008; 134:179–191. [PubMed: 18061179]
30. Nakaya M, Xiao Y, Zhou X, Chang JH, Chang M, Cheng X, et al. Inflammatory T cell responses rely on amino acid transporter ASCT2 facilitation of glutamine uptake and mTORC1 kinase activation. Immunity. 2014; 40:692–705. [PubMed: 24792914]
31. Buck MD, O'Sullivan D, Pearce EL. T cell metabolism drives immunity. J Exp Med. 2015; 212:1345–1360. [PubMed: 26261266]
32. Marzec M, Zhang Q, Goradia A, Raghunath PN, Liu X, Paessler M, et al. Oncogenic kinase NPM/ALK induces through STAT3 expression of immunosuppressive protein CD274 (PD-L1, B7-H1). Proc Natl Acad Sci U S A. 2008; 105:20852–20857. [PubMed: 19088198]
33. Wölfle SJ, Strebovsky J, Bartz H, Sähr A, Arnold C, Kaiser C, et al. PD-L1 expression on tolerogenic APCs is controlled by STAT-3. Eur J Immunol. 2011; 41:413–424. [PubMed: 21268011]
34. Burr ML, Sparbier CE, Chan YC, Williamson JC, Woods K, et al. CMTM6 maintains the expression of PD-L1 and regulates anti-tumour immunity. Nature. 2017; 549:101–105. [PubMed: 28813417]
35. Mezzadra R, Sun C, Jae LT, Gomez-Eerland R, de Vries E, Wu W, et al. Identification of CMTM6 and CMTM4 as PD-L1 protein regulators. Nature. 2017; 549:106–110. [PubMed: 28813410]
36. Garon EB, Rizvi NA, Hui R, Leighl N, Balmanoukian AS, et al. Pembrolizumab for the treatment of non-small-cell lung cancer. N Engl J Med. 2015; 372:2018–2028. [PubMed: 25891174]
37. Rosenberg JE, Hoffman-Censits J, Powles T, van der Heijden MS, Balar AV, Necchi A, et al. Atezolizumab in patients with locally advanced and metastatic urothelial carcinoma who have progressed following treatment with platinum-based chemotherapy: a single-arm, multicentre, phase 2 trial. Lancet. 2016; 387:1909–1920. [PubMed: 26952546]
38. Zhan H, Ma Y, Lin CH, Kaushansky K. JAK2V617F-mutant megakaryocytes contribute to hematopoietic stem/progenitor cell expansion in a model of murine myeloproliferation. Leukemia. 2016; 12:2332–2341.
39. Koopmans SM, Schouten HC, van Marion AM. Anti-apoptotic pathways in bone marrow and megakaryocytes in myeloproliferative neoplasia. Pathobiology. 2014; 81:60–68. [PubMed: 24280934]
40. Yang H, Bueso-Ramos C, DiNardo C, Estecio MR, Davanlou M, Geng QR, et al. Expression of PD-L1, PD-L2, PD-1 and CTLA4 in myelodysplastic syndromes is enhanced by treatment with hypomethylating agents. Leukemia. 2014; 28:1280–1288. [PubMed: 24270737]
41. Davids MS, Kim HT, Bachireddy P, Costello C, Liguori R, Savell A, et al. Ipilimumab for Patients with Relapse after Allogeneic Transplantation. N Engl J Med. 2016; 375:143–153. [PubMed: 27410923]

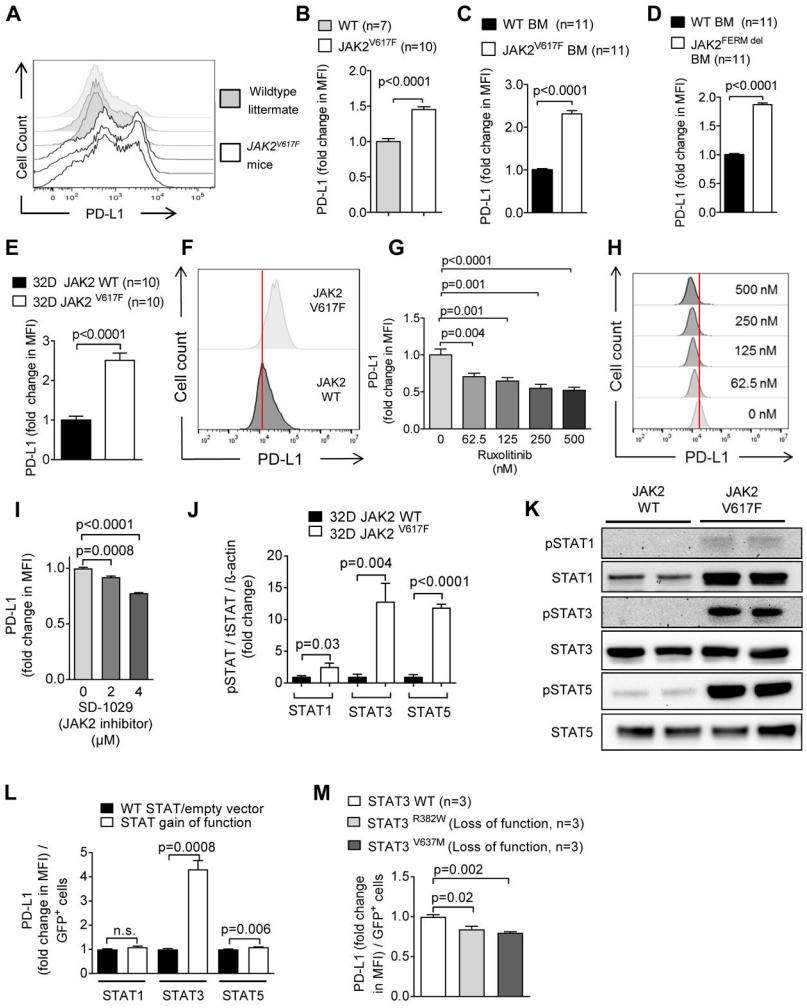

Fig. 1. JAK2 ^{V617F} activation increases PD-L1 expression in myeloid cells

(A) The representative histograms show the expression of PD-L1 on CD41^{+} platelets from the spleens of wildtype littermate mice (gray, n=3) and JAK2^{V617F} mice (white, n=3). One of three independent experiments is shown.

(B) The bar diagrams show fold change of PD-L1 expression on CD41^{+} platelets isolated from the spleens of wildtype littermate and JAK2^{V617F} mice. Data are pooled from two independent experiments (WT littermate mice, n=7; JAK2^{V617F}mice, n=10).

(C, D) The bar diagrams show PD-L1 expression in murine primary BALB/c BM cells isolated from mice on day 4 after treatment with 5-FU, after infection with either GFP $^{+}$JAK2^{V617F} virus **(C)** or GFP^{+}-JAK2 virus (deletion of the FERM inhibitory domain) **(D)**. Data are pooled from 11 technical replicates.

(E) The bar diagram shows PD-L1 expression on 32D cells expressing JAK2 wildtype (JAK2-WT, black) or JAK2^{V617F} (white). Data are pooled from three independent experiments, n=10 each group.

(F) The representative histograms show PD-L1 expression on 32D JAK2-WT cells (dark gray) or 32D JAK2^{V617F} cells (light gray).

(G) The bar diagram shows PD-L1 expression on 32D JAK2^{V617F} cells after exposure to ruxolitinib. Data are pooled from three independent experiments.

(H) The representative histograms show PD-L1 expression on 32D JAK2^{V617F} cells after exposure to different concentrations of ruxolitinib.

(I) The graph shows PD-L1 expression on 32D JAK2^{V617F} cells exposed to the specific JAK2 inhibitor SD-1029. Data (n=4 per group) from one of three independent experiments with comparable results are shown.

(J) The bar diagram indicates the ratio of pSTAT1/STAT1/β-actin, pSTAT3/STAT3/β-actin, and pSTAT5/STAT5/β-actin for 32D JAK2-WT or JAK2^{V617F} cells. Pooled data (n=4 per group) from two independent experiments.

(K) The Western blots display STAT1, STAT3, and STAT5 total protein and phospho-STAT1, phospho-STAT3, and phospho-STAT5 in 32D-JAK2-WT or 32D-JAK2^{V617F} cells. The blots are representative of two independent experiments.

(L) The bar diagram displays the fold change of PD-L1 expression (flow cytometry) on 32D cells that were transfected with a vector containing STAT1 (R321G), STAT3 (Y640F), or STAT5 (S711F) with activating mutations (GOF) or the respective WT STATs (for STAT1/STAT3) or empty vector (STAT5). One representative (n=3 each group) of two independent experiments is displayed.

(M) The bar diagram displays the fold change of PD-L1 expression (flow cytometry) on 32D^{V617F} cells that were transfected with a vector containing two different STAT3 loss-of-function mutations (R382W/V637M). Pooled data from two independent experiments (n=3 per group).

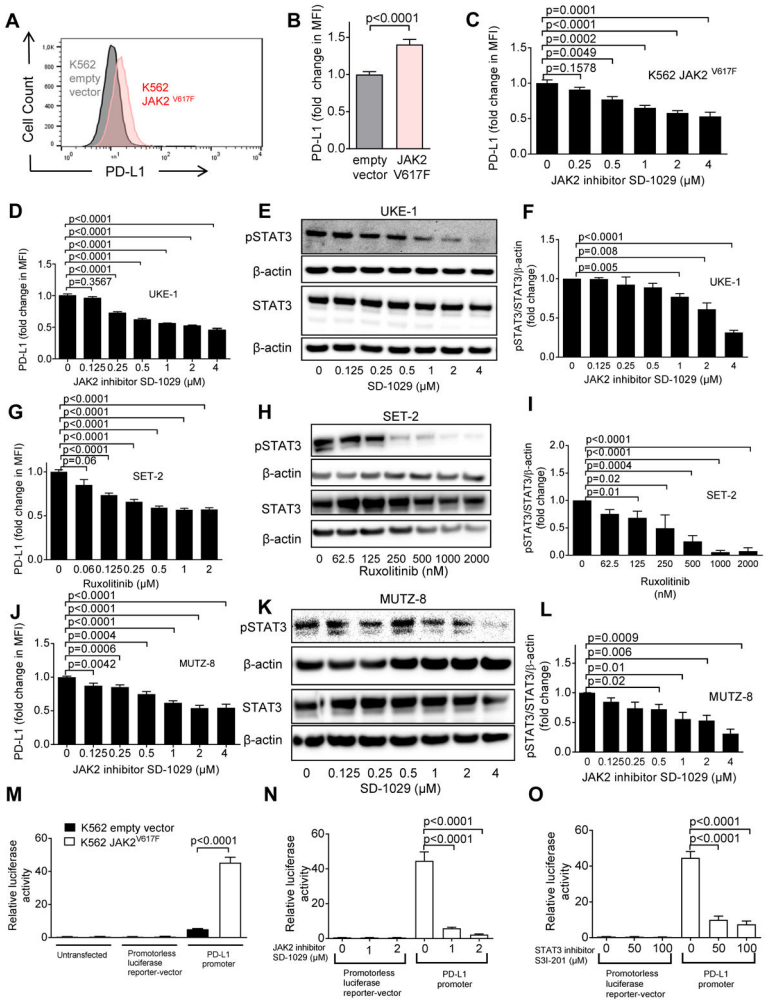

Fig. 2. The mutation JAK2^{V617F} promotes *de novo* PD-L1 gene transcription in human cells

(A) The histograms show the MFI for PD-L1 on K562 cells (transfected with empty vector or JAK2^{V617F} vector). One representative experiment of three experiments with a comparable pattern is shown. The analysis was done on GFP^{+} sorted cells within 3 days after transfection.

(B) The bar diagram displays the fold change of PD-L1 expression (flow cytometry) on K562 cells transfected with empty vector or with JAK2^{V617F}. The data are pooled from 4 independent experiments (n=12 per group).

(C) The bar diagram displays the fold change of PD-L1 expression (flow cytometry) on K562 JAK2^{V617F} cells that were exposed to different concentrations of the JAK2 inhibitor SD-1029. Pooled data from two independent experiments (n=6 at each concentration).

(D) The bar diagram displays the fold change of PD-L1 expression (flow cytometry) for the JAK2^{V617F}-positive cell line UKE-1 treated with the JAK2 inhibitor SD-1029 (n=7 at each concentration).

(E) The Western blots display STAT3 total protein, β-actin and phospho-STAT3 in UKE-1 cells being treated with the JAK2 inhibitor SD-1029. The blots are representative of three independent experiments.

(F) The bar diagram indicates the ratio of pSTAT3/STAT3/β-actin (normalized to 1 in the condition without JAK2 inhibitor) for the cells described in (E). Pooled data from three replicates (n=3 for each concentration).

(G) The bar diagram displays the fold change of PD-L1 expression (flow cytometry) for $JAK2^{V617F}$ positive cell line SET-2 treated with ruxolitinib. Pooled data from three independent experiments (concentration 0 – 0.5 μM: n=12, concentration 1 and 2 μM: n=6).

(H) The Western blots display STAT3, β-actin, and phospho-STAT3 in SET-2 cells being treated with ruxolitinib. The blots are representative of three independent experiments.

(I) The bar diagram indicates the pSTAT3/STAT3/β-actin ratio for cells described in (H). Pooled data from three independent experiments (n=3 for each concentration).

(J) The bar diagram displays the fold change of PD-L1 expression (flow cytometry) for $JAK2^{V617F}$ positive cell line MUTZ-8 that was treated with the JAK2 inhibitor SD-1029 (n=3 for each concentration).

(K) The Western blots display STAT3 total protein, β-actin and phospho-STAT3 in MUTZ-8 cells being treated with the JAK2 inhibitor SD-1029. The blots are representative of three independent experiments.

(L) The bar diagram indicates the ratio of pSTAT3/STAT3/β-actin for cells described in (K). Pooled data from three independent experiments (n=3 for each concentration).

(M) The bar diagram indicates the relative luminescence activity of K562 cells (containing empty vector or $JAK2^{V617F}$) which were left untransfected or transfected with either a promoterless luciferase reporter-vector pgl4.13 or a reporter vector containing the PD-L1 promoter. Pooled data from three technical replicates (n=6 for each condition).

(N) The bar diagram indicates the relative luciferase activity of K562 $JAK2^{V617F}$ cells transfected with either the promoterless luciferase reporter vector pgl4.13 or the reporter vector containing the PD-L1 promoter and treated with the JAK2-inhibitor SD-1029. Pooled data from three independent experiments (n=6 for each condition).

(O) The bar diagram indicates the relative luminescence activity of K562 $JAK2^{V617F}$ cells transfected with either the promoterless luciferase reporter vector pgl4.13 or the reporter vector containing the PD-L1 promoter and treated with the STAT3 inhibitor S3I-201. Pooled data from three independent experiments (n=6 for each condition).

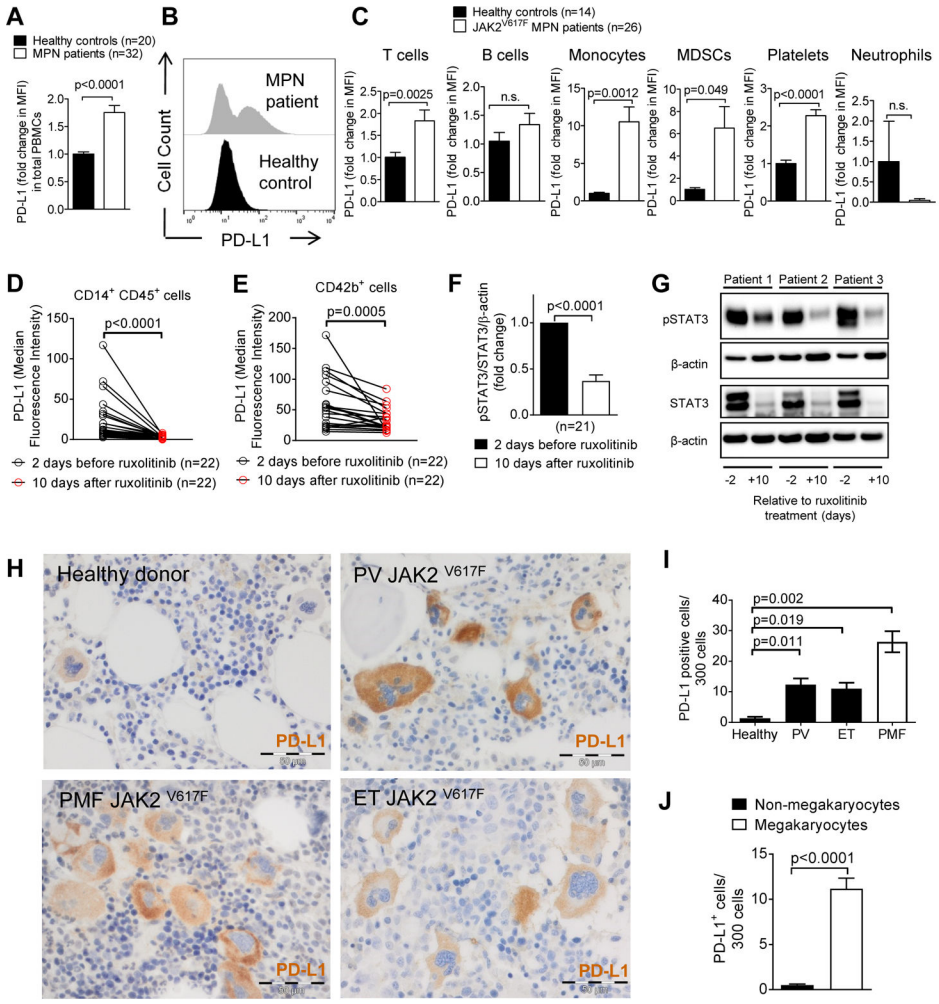

Fig. 3. PD-L1 is expressed on different cell types in MPN patients

(A) The bar diagram indicates the expression of PD-L1 on peripheral blood cells and platelets from healthy volunteers or MPN patients.

(B) The histograms show PD-L1 expression on peripheral blood cells and platelets in healthy individuals or MPN patients as described in **(A)**.

(C) The bar diagrams show PD-L1 expression in different cell types: T cells ($CD3^+$), B cells ($CD19^+$), monocytes ($CD11b^+CD14^+$), MDSCs ($CD11b^+CD33^+CD14^-$), platelets ($CD42b^+$), and neutrophils ($CD11b^+CD15^+$) from multiple MPN patients and healthy controls. Data were normalized to the PD-L1 MFI of healthy controls set as 1.

(D, E) The diagrams show PD-L1 expression (MFI) in $CD14^+$ monocytes (**D**) and $CD42b^+$ platelets (**E**) from MPN patients on day 2 before ruxolitinib-treatment and 10 days after start of ruxolitinib. Each data point indicates the measurement of an individual patient at the indicated time point. The *P* value was determined by using the Wilcoxon matched-pairs signed rank test.

(F) The bar diagram shows the pSTAT3/STAT3/β-actin ratio within PBMCs from MPN patients on day 2 before ruxolitinib treatment and 10 days after start of ruxolitinib. Pooled results from 21 patients.

(G) The Western blots show pSTAT3 and STAT3 protein amounts within PBMCs from 3 representative MPN patients on day 2 before ruxolitinib treatment and 10 days after start of ruxolitinib.

(H) Displayed are representative BM biopsies from a healthy control and different MPN patients with verified $JAK2^{V617F}$ mutations. $PD\text{-}L1^{+}$ cells appear in brown. The scale bar represents 50 μm.

(I) The bar diagram displays the number of $PD\text{-}L1^{+}$ cells out of 300 cells detected in BM biopsies from healthy volunteers or from multiple patients with the indicated MPN type. PV: polycythemia vera, ET: essential thrombocythemia, PMF: primary myelofibrosis.

(J) The bar diagram displays the number of $PD\text{-}L1^{+}$ megakaryocytes versus all $PD\text{-}L1^{+}$ non-megakaryocyte cells detected out of 300 cells examined in BM biopsies of patients with JAK2-mutant MPN. Data are pooled from 39 patients.

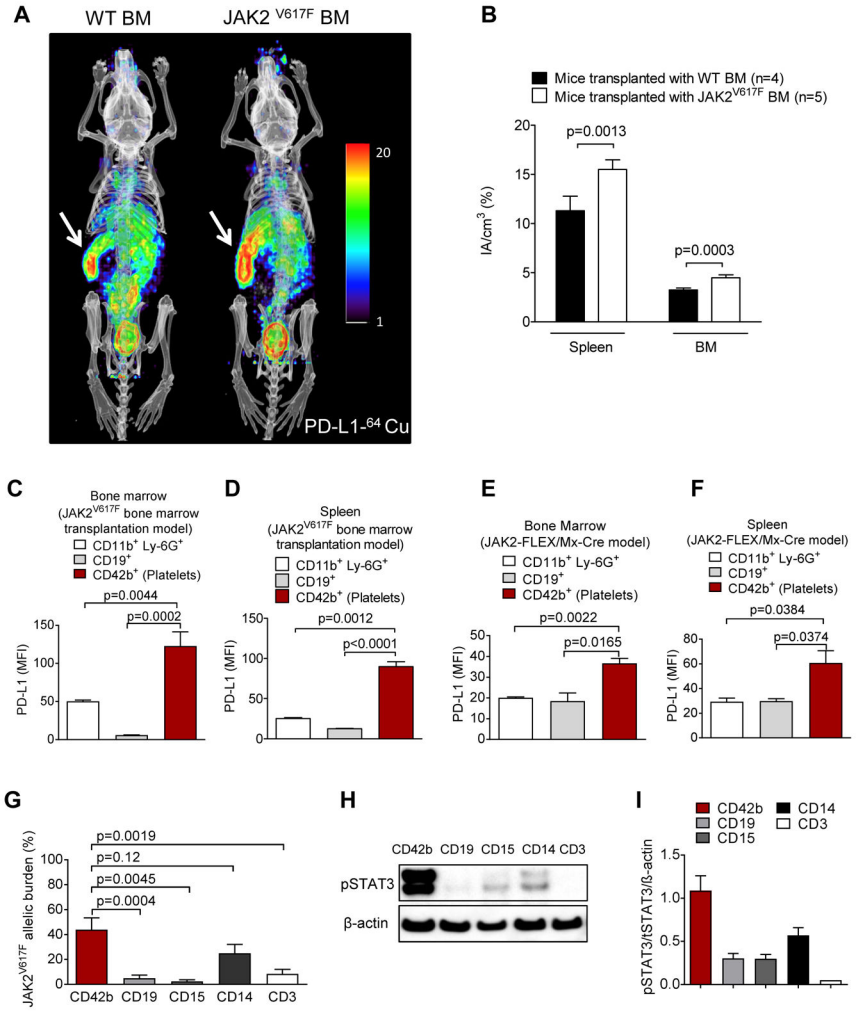

Fig. 4. PD-L1 expression is found in the spleen and the bone marrow of mice transplanted with JAK2^{V617F} transduced bone marrow

(A) Two representative mice imaged by PET/CT using a ^{64}Cu-labeled anti-PD-L1 antibody are shown. BALB/c mice had received either JAK2^{V617F}-transfected (right) or WT syngeneic BM (left) after total body irradiation (TBI, 6.5 Gy). The signal intensity indicates areas with high PD-L1 expression. Arrows point towards the spleen (high signal intensity). The image is representative of 4 mice per group with comparable signal patterns.

(B) The bar diagram shows the signal intensity in the indicated organs of mice transplanted as described in **(A)**. Data are pooled from 4 or 5 mice per group.

(C, D) The bar diagram shows the MFI for PD-L1 on different cells and platelets in the BM (**C**) or spleen (**D**) of mice transplanted as described in **(A)**. n=5 each group.

(E, F) The bar diagram shows the MFI for PD-L1 on different cells and platelets in BM (**E**) and spleen (**F**) of JAK2-FLEX/Mx-Cre mice (n=3 each group).

(G) The bar diagram shows the JAK2^{V617F} allele burden in different cell populations isolated by cell sorting from 15 MPN patients. The JAK2^{V617F} allele burden was determined by qPCR (n=15 each group).

(H) The Western blot shows the amounts of pSTAT3 and STAT3 in different cell populations isolated by cell sorting from a representative polycythemia vera patient.
(I) The bar diagram shows the ratios of pSTAT3/STAT3/β-actin in different cell populations isolated by cell sorting from multiple MPN patients (n=5 for CD42b, CD19, CD15, and CD3, n=3 for CD14).

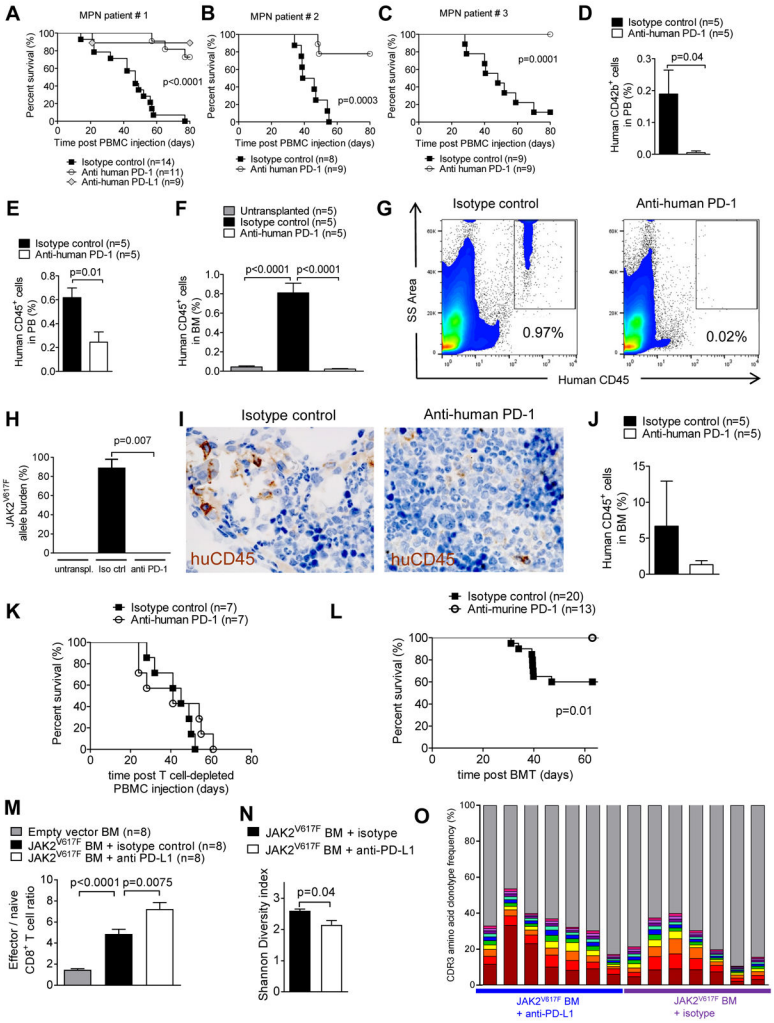

Fig. 5. PD-1 blockade improves survival in MPN mouse models

(A–C) The survival of *RAG2*$^{-/-}$*Il2r*$^{-/-}$ mice after intravenous transfer of human PBMCs from patient #1 (A), patient #2 (B), and patient #3 (C) (table S2) is shown. Mice were treated with 250 μg of either isotype-control Ab, or anti-human PD-1 Ab, or anti-human PD-L1 Ab on day 8 after PBMC injection. Pooled data from three independent experiments.

(D, E) The bar diagram shows the percentage of human CD42b^{+} platelets (**D**) or human CD45^{+} cells (**E**) in the peripheral blood of *RAG2*$^{-/-}$*Il2r*$^{-/-}$ mice transplanted with PBMCs from MPN patient #1. The analysis was performed on day 21 after intravenous transfer of human PBMCs.

(F) The bar diagram shows the percentage of human CD45^{+} cells determined by flow cytometry in the BM of untreated *RAG2*$^{-/-}$*Il2r*$^{-/-}$ mice. *RAG2*$^{-/-}$*Il2r*$^{-/-}$ mice had received intravenous transfer of human PBMCs from patient #1 (table S2) and were treated with isotype Ab or anti-human-PD-1 (250 μg, day 8). The analysis was performed on day 39 after intravenous transfer of human PBMCs.

(G) Representative FACS plots showing the percentage of human CD45^{+} cells in BM of *RAG2*$^{-/-}$*Il2r*$^{-/-}$ mice transplanted and treated as described in (**F**).

(H) The bar diagram shows the JAK2^{V617F} allele burden in BM harvested from *RAG2*$^{-/-}$*Il2r*$^{-/-}$ mice treated as described in (**F**).

(I) Representative pictures of human CD45^{+} cells (brown) in the BM harvested from *RAG2*$^{-/-}$*Il2r*$^{-/-}$ mice treated as described in (**F**). The scale bar size represents 50 μm.

(J) Shown is the quantification of the CD45^{+} cells in BM harvested from *RAG2*$^{-/-}$*Il2r*$^{-/-}$ mice treated as described in (**F**).

(K) Survival of *RAG2*$^{-/-}$*Il2r*$^{-/-}$ mice after intravenous transfer of human PBMCs depleted of CD3^{+} T cells from patient #1 (table S2) is shown. Mice were treated with isotype control or anti-human PD-1 (250 μg) on day 8 after transplantation. Data are pooled from two independent experiments.

(L) Survival of BALB/c mice, which had received JAK2^{V617F}-transfected syngeneic BM after TBI and isotype control Ab or anti-PD-1 Ab. Data are pooled from two independent experiments.

(M) The bar diagrams show the ratio of effector/naive CD8^{+} T cells in spleens isolated from mice described in **(L)** on day 19 after transplantation (each group n=8).

(N) The mean diversity index of TCRα complementarity determining region 3 (CDR3) amino acid sequences for isotype control Ab or anti-PD-1 Ab groups is shown. Error bars represent standard error of the mean.

(O) The abundance of the CDR3 amino acid clonotype frequency of the ten strongest clones according to variable αβ-TCR genes for isotype control Ab or anti-PD-1 Ab groups is shown. Each bar represents an individual mouse; different colors display different clones.

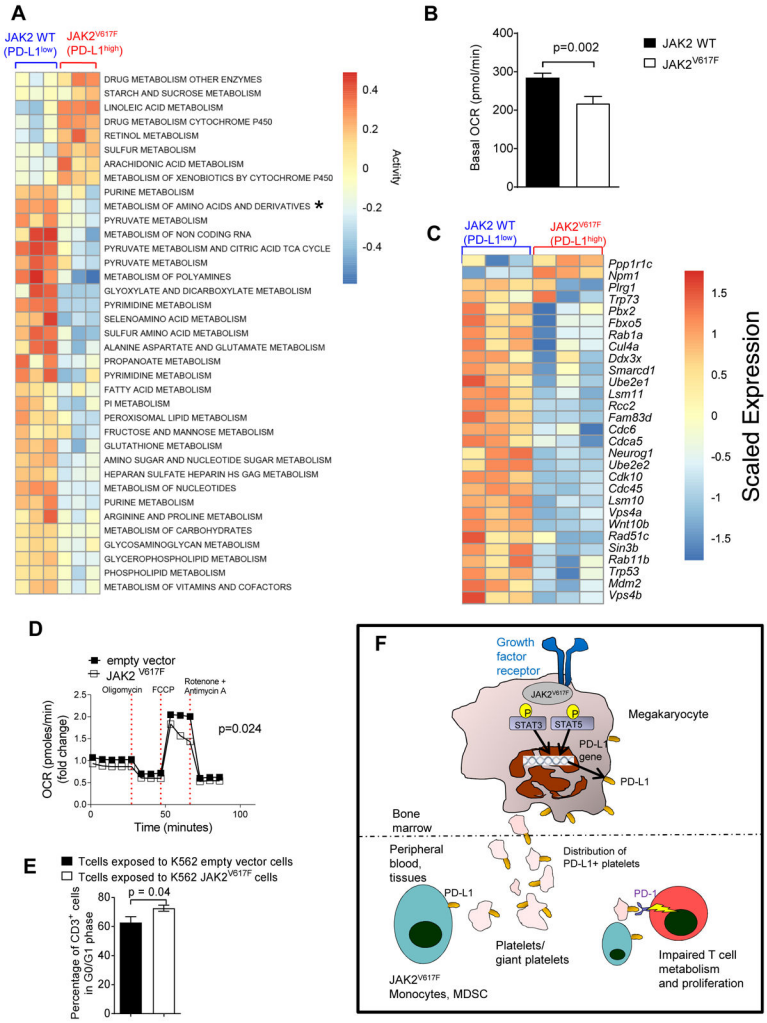

Fig. 6. JAK2^{V617F}-mutant cells affect metabolism and cell cycle in T cells

(A) The heat map depicts the activity scores of differentially regulated metabolic pathways in T cells (C3H) that were exposed to JAK2^{V617F}-mutant or JAK2-WT 32D cells (C3H) for 24 hours (n=3 empty vector, n=3 JAK2^{V617F}-mutant 32D cells). The asterisk indicates the metabolism of amino acids and derivatives for this metabolic pathway for which the groups are significantly different (adjusted $P < 0.005$). Pathways were selected from KEGG and Reactome gene sets containing the word “Metabolism”.

(B) Basal OCR of mouse CD3^{+} T cells (C3H) that were exposed to 32D JAK2^{V617F} or 32D JAK2-WT cells (C3H) for 24 hours. Data were combined from 3 independent biological repeats.

(C) The heat map depicts genes from the GO term “Positive Regulation of Cell Cycle Phase Transition” that have an absolute log2 fold change >0.1 between T cells (C3H) that were exposed to JAK2^{V617F} mutant or JAK2-WT 32D cells (C3H) for 24 hours (n=3 JAK2-WT and n=3 JAK2^{V617F}-mutant 32D cells).

(D) Time course for OCR of human CD3^{+} T cells that were exposed to human K562 cells with a JAK2^{V617F} mutation (or K562 cells with empty vector) for 24 hours at baseline and

after oligomycin (Oligo), FCCP, and rotenone plus antimycin A (R+A) exposure. Data were combined from 2 experiments.

(E) The bar diagram represents the percentage of human $CD3^+$ cells that were in G0/G1 phase (non-cycling) when T cells were exposed for 24 hours to K562 $JAK2^{V617F}$ cells (or K562 cells with empty vector). The data are pooled from 2 independent experiments (n=10 each group).

(F) Proposed mechanism of JAK2-mediated immune escape in MPN: Greater JAK2 activity increases STAT3 and STAT5 phosphorylation. pSTAT3 and pSTAT5 bind to and activate the PD-L1 promoter, resulting in PD-L1 transcription and consequently higher PD-L1 surface expression. Platelets derived from neoplastic ($JAK2^{V617F}$) megakaryocytes, as well as monocytes and MDSCs, all express PD-L1 abundantly and are distributed via the peripheral blood, which causes T cell exhaustion via interaction of PD-L1 on the platelets and myeloid cells with PD-1 on T cells.